

Catalytic and non-catalytic low-pressure hydrothermal liquefaction of pinewood sawdust, polyolefin plastics and their mixtures

Jude A. Onwudili^{a,b,*}, Paul T. Williams^c

^a Energy and Bioproducts Research Institute, School of Infrastructure & Sustainable Engineering, College of Engineering and Physical Sciences, Aston University, Birmingham, B4 7ET, UK

^b Department of Chemical Engineering & Applied Chemistry, School of Infrastructure & Sustainable Engineering, College of Engineering and Physical Sciences, Aston University, Birmingham, B4 7ET, UK

^c School of Chemical and Process Engineering, The University of Leeds, Leeds, LS2 9JT, UK

ARTICLE INFO

Handling Editor: Maria Teresa Moreira

Keywords:

Low-pressure co-hydrothermal liquefaction
Catalyst
Plastic wastes
Biomass
Hydrocarbon-rich fuel

ABSTRACT

Hydrothermal co-liquefaction of biomass and polyolefin plastic feedstocks offers the advantage of potential synergistic reaction environments for producing liquid products of high fuel quality. In this present study, hydrothermal liquefaction and co-liquefaction of sawdust, low-density polyethylene and high-density polyethylene were investigated in a batch reactor from 350 °C to 450 °C and autogenic pressures below 30 bar. The novel low-pressure hydrothermal processing method was carried out with and without low-cost Ni-Cu/Al₂O₃ bimetallic catalyst. Thermal degradation of the sawdust started at 350 °C, whereas the plastics could only completely degrade at 450 °C, which was then chosen as the optimum reaction temperature. The catalysed process led to an increase in oil yield from the sawdust, with carbon enrichment by 16.3% and 22% deoxygenation. Furthermore, the catalyst promoted the formation of ketones and aromatic hydrocarbons, while consuming phenols and furfural in the sawdust-derived bio-oils. For the plastics, the catalyst, gave slight decreases in oils yield in favour of gas and/or char formation, with the promotion of *in situ* hydrogenation to enhance the yields of alkanes over alkenes. Results from hydrothermal co-liquefaction tests showed that synergistic interactions occurred between the degradation products of sawdust and the plastics. The observed synergy was further promoted by the presence of the catalyst, leading to dramatic deoxygenation of the oil products to produce hydrocarbon-rich fuels with less than 4 wt% oxygen contents (≈90% deoxygenation). This low-pressure hydrothermal co-liquefaction process is an efficient and cost-effective pathway for single-loop conversion of widely available biomass and plastics feedstocks into highly deoxygenated oils for use as sustainable fuels.

1. Introduction

Production of alternative liquid fuels and chemicals from organic solid waste materials such as waste plastics and biomass has many benefits for society. With desirable properties like lightweight, high strength, durability and ease of moulding, plastics have become common materials for daily life. Annual production of plastics currently stands at over 400 million tonnes (Geyer et al., 2017). However, with their short service life, the accumulation of large quantities of waste plastics has become a major environmental pollution problem. Among plastics, hydrocarbon-only polyolefin plastics (polyethylene, polypropylene and polystyrene) together account for more than 70% of plastic wastes (Onwudili et al., 2009) with polyethylenes and

polypropylene accounting to 50% (Faust et al., 2023). Chemical recycling of these polyolefins via thermochemical conversion to fuels and chemicals is one of the potentially viable options for managing these plastic wastes. In addition, thermochemical conversion of solid non-food (lignocellulosic) biomass into fuels and chemicals has been recognised as a sustainable pathway to the defossilisation of the carbon-based energy and chemicals sector (Zhang et al., 2013; Liu and Yu, 2022).

Direct conversion of organic solid feedstocks into liquid fuels and chemicals can be achieved via technologies such as pyrolysis and hydrothermal liquefaction (HTL) (Bhaskar et al., 2002; Zhang et al., 2013; Sharma et al., 2021). Both pyrolysis and HTL involve the application of heat to thermally degrade polymeric materials into smaller, simpler molecules, with or without added catalysts, aiming to produce oils.

* Corresponding author. Energy and Bioproducts Research Institute, School of Infrastructure & Sustainable Engineering, College of Engineering and Physical Sciences, Aston University, Birmingham, B4 7ET, UK.

E-mail address: j.onwudili@aston.ac.uk (J.A. Onwudili).

<https://doi.org/10.1016/j.jclepro.2023.139733>

Received 24 August 2023; Received in revised form 28 October 2023; Accepted 10 November 2023

Available online 13 November 2023

0959-6526/© 2023 The Authors. Published by Elsevier Ltd. This is an open access article under the CC BY license (<http://creativecommons.org/licenses/by/4.0/>).

However, HTL is highly suitable for processing wet organic wastes and materials, thereby saving substantial energy costs from intensive drying required by pyrolysis. In addition, HTL uses hot-pressurised water medium, which has unique properties that promote fast reaction and mass transfer rates (Özgen, 2020; Lachos-Perez et al., 2022). HTL can be carried out in subcritical water (250 °C–374 °C, up to 221 bar) mostly for biomass (Elliott et al., 2015) and within the supercritical water region (>374 °C, >224 bar) for polyolefin plastics (Mukundan et al., 2022; Laredo et al., 2023), due to different types and strengths of bonds present in the covalent structures of the respective feedstocks. For instance, HTL of polypropylene at 350 °C without a catalyst produced 83 wt% solid (Sebestyén et al., 2022). However, when the conditions were increased to supercritical conditions of 425 °C, 91 wt% of oil, comprising of 80% naphtha was obtained after 2 h–4 h of reaction, with similar results using reduced reaction times of 0.5 h–1 h at 450 °C (Sebestyén et al., 2022).

Hydrothermal co-liquefaction (co-HTL) of biomass with waste plastics can inhibit char-forming reactions and promote *in situ* deoxygenation of bio-oils to enhance the yields of hydrocarbon-rich liquid fuels (Mukundan et al., 2022). For example, oil products with less than 15 wt % oxygen content compared to bio-oil have been reported using co-processing of biomass and plastics (Hongthong et al., 2020b). Since plastics have much higher H/C ratio than biomass, their degradation products can act as intermediate active reactants and hydrogen donors for *in situ* upgrading of bio-oils (Jahirul et al., 2012; Wagner et al., 2016; Watson et al., 2020). Essentially, the oil product from plastic can become a carrier for the biomass degradation products, promote heat distribution, prevent local hotspots, and minimise char formation. Hence, the components in the oils from biomass and plastics can interact synergistically leading to a composite oil with improved fuel properties (Yuan et al., 2009; Mukundan et al., 2022).

The presence of catalysts during co-HTL of biomass and plastics have been found to be beneficial (Mukundan et al., 2022; Luna-Murillo et al., 2021; Stanton et al., 2018; Hongthong et al., 2020a; Hongthong et al., 2020b). For example, the use of aluminosilicate catalyst doubled the oil yield during the co-HTL of a 50:50 mixture of polypropylene (PP) plastic with pistachio hulls compared to the non-catalytic test (Hongthong et al., 2020a). Also, Mukundan et al. (2022), conducted catalytic co-HTL of *prosopis juliflora* biomass and PP plastics using alumina supported metal oxides (Mo, Ni, W, and Nb) catalysts. At biomass to plastic mass ratio of 3:1, the authors reported that Nb/Al₂O₃ catalyst led to the highest yield of partially deoxygenated oil product (46.5 wt%) (Mukundan et al., 2022). Hence, improving the yields and quality of oil products during co-HTL of plastics and biomass with cheap catalysts remains an important research topic to ensure process viability.

However, one of the challenges of co-HTL of biomass and plastics is that the conversion of each feedstock occurs within different temperature (and pressure) ranges in the hydrothermal media. As mentioned earlier, unlike HTL of biomass, which is accomplished in subcritical water, the degradation of polyolefins requires supercritical water conditions to provide sufficient activation energy for the reaction. Supercritical water processing involves high pressures (above the critical pressure of water of 221 bar). Therefore, recent successful studies on co-HTL of biomass and plastics have been reported with operating pressures of 200 bar and above (Chen et al., 2019; Seshasayee and Savage, 2021; Mukundan et al., 2022). Operating at such pressures have implications of high processing costs. Recently, Jin et al. (2021) reported a low-pressure hydrothermal processing (LT-HTP) method for conversion of plastics into fuel oils as a way of reducing processing costs. The authors achieved 87 wt% oil from mixed polyolefin feedstock at 450 °C after 45 min of reaction. For plastic conversion to fuel oil, Jin et al. (2021) reported that LP-HTP could lower capital costs by 90 % and deliver 80% energy savings compared to high-pressure supercritical water processing. Applying such a process to co-HTL of biomass and plastics could provide similar benefits of reduced processing costs, in addition to the prospects of obtaining oil products with better fuel

properties than bio-oils.

In this present work, non-catalytic and catalytic HTL and co-HTL of sawdust (SD) biomass and virgin low-density polyethylene (LDPE) and high-density polyethylene (HDPE) were investigated under low-pressure hydrothermal liquefaction (LP-HTL) conditions. LP-HTL can enable the co-HTL of biomass and plastics at sufficiently high temperatures, allowing for the degradation of both types of feedstocks. The aim was to promote synergistic interactions, leading to high-quality liquid fuel production at arguably lower costs than high-pressure HTP systems. To further enhance the formation of deoxygenated oils, an alumina-supported bimetallic nickel-copper catalyst (Ni–Cu/Al₂O₃), previously reported to promote deoxygenation and *in-situ* hydrogenation reactions (Alves and Onwudili, 2022) was selected for this present work. The yields of products and detailed analyses of oil products were used to evaluate the synergistic effects from the co-HTL of SD and plastics and to establish the plausible reaction pathways leading to the formation of hydrocarbon-rich oil products.

2. Materials and methods

2.1. Materials

SD pellets were obtained from the feedstock storage of the biomass-powered pilot plant at the Energy and Bioproducts Research Institute (EBRI), Aston University, UK. The SD was ground to particle size 5–10 mm before use. LDPE and HDPE, in the forms of spherical pellets, were obtained from Sigma-Aldrich Ltd, UK and used as received. The catalyst used comprised of 10 wt% Ni (as NiO) and 10 wt% Cu (as CuO) on alumina 1 mm spheres (Ni–Cu/Al₂O₃) and was obtained from Catal International Ltd, Sheffield, UK. The catalyst was characterised by nitrogen adsorption/desorption porosimetry to determine the Brunauer-Emmett-Teller (BET) surface area (110.5 m²/g), pore volume (0.23 cm³/g) and pore diameter (6.72 nm). A Micromeritics Tristar 3000 system (Micromeritics, Norcross, GA, USA) was used for these determinations (Razaq et al., 2021). Dichloromethane (DCM) solvent was used to recover and separate the oil product from solid residues after each experimental run. Deionised water was prepared in-house using a Milli-Q Advantage A10 Water Purification System and used for the HTL and co-HTL experiments.

Table 1 shows the characteristics of the feedstocks used in this present study. The carbon, hydrogen and nitrogen compositions of the feedstocks were determined using a Thermo Scientific Flash 2000 elemental analyser while the oxygen content was determined by difference. The ash contents of the feedstocks were determined in a Carbolite AAF 110 furnace, the furnace was heated from room temperature to 650 °C at a rate of 10 °C min⁻¹ and held for 2 h (ASTM 3172). The higher heating values (HHV) of the feedstocks were calculated from their elemental compositions using the method reported by Channiwalla and Parikh (2002). The volatile matter and fixed carbon fractions were determined in a Mettler Toledo thermal analyser heated from 25 to 900 °C at a rate of 10 °C min⁻¹ under high purity nitrogen gas with a flow of 30 ml min⁻¹.

2.2. Experimental

2.2.1. Procedure for HTL and co-HTL experiments

A 75 ml non-stirred batch reactor with temperature and pressure ratings of 600 °C and 345 bar, respectively was used to conduct HTL experiments. The reactor, supplied by Parr Instruments, Illinois, (USA), was fitted with a thermocouple at the bottom and a pressure gauge at the top, for monitoring its temperature and pressure, respectively. Reactions were carried out within a temperature range of 350 °C–450 °C, pressures below 30 bar and reaction times from 0.5 to 4 h to determine the optimum conditions for the co-HTL of individual and mixed feedstocks. For experiments involving individual feedstocks, 2 g of SD, LDPE or HDPE was used, while for experiments involving mixtures of SD and each

Table 1
Elemental and proximate compositions of the feedstocks.

	C (wt.%)	H (wt.%)	N (wt.%)	O ^a (wt.%)	HHV (MJ/kg)	Ash (wt.%)	Moisture content (wt.%)	Volatile matter (wt.%)	^a Fixed carbon (wt.%)
SD	46.61	6.42	0.27	46.7	17.7	2.97	2.55	81.15	13.43
LDPE	85.08	14.84	0.08	–	49.0	0.03	0.02	99.05	–
HDPE	84.90	15.01	0.09	–	49.2	–	0.03	99.97	–

^a calculated by difference.

plastic (SD/LDPE and SD/HDPE), 1 g of SD and 1 g of each plastic were used). For catalytic experiments, 1.0 g of Ni–Cu/Al₂O₃ catalyst was mixed with the feedstock inside the reactor. To provide the low-pressure hydrothermal environment, 10 mL of deionised water was added into the reactor, followed by sealing and purging with nitrogen gas for 10 min. Thereafter, the loaded reactor was placed in a 3-kW ceramic

(≈20 mL). This was transferred a pre-weighed 100 mL conical flask and placed on a hotplate maintained at 40 °C to discharge the DCM solvent. The sample was removed from the hotplate once visible condensation of liquid at the neck of the conical flask was no longer observed. The flask was sealed with pre-weighed parafilm, cooled in a desiccator, and weighed. The yields of oil products were calculated using Equation (3).

$$\text{Yield of oil, (wt\%)} = \frac{(\text{mass of conical flask and oil product} - \text{mass of conical flask})}{\text{mass of feedstock used}} \times 100 \quad (3)$$

knuckle heater controller and heated at an average of 10 °C min⁻¹ to the desired temperature. In each experiment, the reaction time was read when the reactor reached the desired temperature. The heating time, which varied depending on the desired temperature (30–40 min) was not included in the reported reaction time. The 10 mL of water used in the reactions ensured that the reported autogenic pressures generated from the expansion of water (Yuan et al., 2009), and to a lesser extent, by the formation of gas products remained safely below 30 bar. After the desired conditions were reached, heating was stopped, and the reactor withdrawn from the heater to cool to ~25 °C using a laboratory fan in under 30 min.

2.2.2. Mass balances

The mass of gas products formed during the reactions was determined by weighing the complete reactor before and after gas discharge (Kohansal et al., 2021) and used to calculate the gas yield according to Equation (1).

$$\text{Yield of gas (wt\%)} = \frac{M_1 - M_2}{\text{mass of feedstock used}} \times 100 \quad (1)$$

Where:

M_1 = mass of reactor before gas discharge.

M_2 = mass of reactor after gas discharge.

Thereafter, the remaining reactor contents (solids and liquids) were collected using 20 mL of DCM solvent. The mixture of solids, reactor liquids (water and oil) and DCM was passed through a Whatman No. 1 filter paper under vacuum to recover the solid residues. The mass of the solid residues was determined by weighing after drying to a constant mass in an oven at 105 °C, for up to 2 h. The yields of solid residues were calculated using Equation (2).

$$\text{Yield of solid residue (wt\%)} = \frac{\text{mass of solid recovered} - \text{mass of catalyst used}}{\text{mass of feedstock used}} \times 100 \quad (2)$$

The mixture of DCM and oil (organic layer) was separated from the aqueous phase using a 100 mL separating funnel. The organic layer was dried over anhydrous sodium sulphate and the final volume measured

For samples involving SD at lower processing temperatures and/or short reaction times, the aqueous layers gave brownish colours. Hence where applicable, the aqueous layers (≈10 mL) were transferred into pre-weighed porcelain crucibles to evaporate off the water on a water-bath. The porcelain crucible and any solid residual present were placed in an oven at 105 °C and dried to a constant weight. These solid residuals were denoted here as water-soluble products (WSPs) and their yields calculated using Equation (4).

$$\text{Yield of WSP (wt\%)} = \frac{\text{mass of crucible and solid residuals} - \text{mass of crucible}}{\text{mass of feedstock used}} \times 100 \quad (4)$$

It is important to note here that the aqueous layers obtained from experiments at higher temperatures (≥400 °C) and longer reaction times were clear and colourless. Some of these were tested for WSPs and found to contain none.

The yields of each product from the co-HTL of SD/LDPE and SD/HDPE mixtures, respectively, were further evaluated for synergistic effects using Equation (5) (Mukundan et al., 2022).

$$\text{Synergy factor (product yields)} = \frac{\text{Experimental Yield} - \text{Calculated Yield}}{\text{Calculated Yield}} \quad (5)$$

The calculated yield of each reaction product was obtained using Equation (6) based on their yields from the HTL of individual feedstock.

$$\text{Calculated Yield (wt\%)} = (x_{\text{Sawdust}} \times Y_{\text{Sawdust}}) + (x_{\text{Plastic}} \times Y_{\text{Plastic}}) \quad 6$$

where.

x = mass fraction; Y = wt%yield; Plastic = LDPE or HDPE (as appropriate).

2.2.3. GC/MS analysis of organic liquid products

The organic liquid product obtained from selected experiments (at

optimum conditions) were analysed using a Shimadzu GC-2010 GC/MS with electron impact ionisation (70 eV) (Onwudili and Scaldasferri, 2023). In this procedure, each oil product was redissolved in DCM to the same volume (30 ml) for the GC/MS analysis. Then, 1 μ L of the diluted sample was introduced at a split ratio of 1:20 into the injector, which was maintained at 300 °C. An RTX-5ms capillary column (internal diameter = 0.25 mm, length = 30 m) was used for the separation with helium at a flow rate of 15 mL min⁻¹ as the carrier gas. The initial column oven temperature was 50 °C, held for 5 min before being heated at a rate of 2.5 °C min⁻¹ to 185 °C. It was then heated further with a rate of 5 °C min⁻¹ to 280 °C and held for 10 min. The total run time was 88 min. The NIST (National Institute of Standards and Technology) Library present on the MS was used to identify the various organic components in the organic liquid. Peak area percent was calculated to achieve semi-quantitation according to Equation (7) (Xu et al., 2013; Ahmadi et al., 2017; Seshasayee and Savage, 2021). Hence, by diluting all samples to the same volume the peak areas of compounds from the GC/MS analysis were deemed to be proportional to their concentrations in the oil respective products.

$$\text{Component A peak area \%} = \frac{\text{peak area of component A}}{\sum \text{peak areas of all components}} \times 100 \quad 7$$

Following GC/MS analysis, the compounds in the oils were categorised into ketones, alkanes, alkenes, aromatic hydrocarbons, furfural, furans, carboxylic acids, phenols, and others. The 'others' refer to minor compounds (>1 %) that did not fit into these main categories). The possibility of synergistic interactions the reaction intermediates from SD and the plastics for the reactions at 450 °C, were evaluated using Equation (8).

$$\text{Synergy factor (oil compositions)} = \frac{\text{Experimental Peak Area \%} - \text{Calculated Peak Area \%}}{\text{Calculated Peak Area \%}} \quad 8$$

The Calculated Peak Area % of each compound class was obtained using Equation (9) for oils from both the individual and mixed feedstocks obtained from experiments at 450 °C for 1 h, which was identified as the optimum condition, when complete conversion of all three feedstocks occurred.

$$\text{Calculated Peak Area \%} = (x_{\text{Sawdust}} \times \text{PA}_{\% \text{Sawdust}}) + (x_{\text{Plastic}} \times Y_{\text{Plastic}}) \quad 9$$

where,

x = mass fraction; $\text{PA}_{\%}$ = peak area% of each compound class in SD and LDPE or HDPE oils.

3. Results and discussions

3.1. Influence of temperature on product yields from non-catalytic HTL of individual feedstocks

Non-catalytic HTL of individual feedstocks (SD, LDPE and HDPE) were carried out to investigate the effects of reaction temperatures on the yields of products from 350 °C to 450 °C for 1 h reaction time. The results of the are presented in Table 2, showing mass balance closures greater than 96 wt%. Table 2 shows that degradation of the SD feedstock occurred even at the lowest temperature of 350 °C used in this work. This agreed with reports in literature, which indicated that HTL of biomass to mostly char and oil normally occurred around 250 °C to about 370 °C (Elliott et al., 2015; Gollakota et al., 2018). The yields of gas products from SD increased with increasing temperature from 11.6 wt% at 350 °C to 15.3 wt% at 450 °C. These results showed that most of the gas forming reactions for SD were occurring at 350 °C, without dramatic increases as temperature increased. Qualitative analysis of the gas products using GC/TCD and GC/FID (Razaq et al., 2021) showed that the gas products from SD were consistently dominated by CO₂ (>85 %), followed by CO, methane, ethane and propane (Yuan et al., 2009; Caprariis et al., 2020).

In addition, oil yields from SD increased nearly three times from 350 °C to 400 °C. Interestingly, a decrease in the amount of solid residue recovered was observed by increasing the temperature from 350 °C to 400 °C, which corresponded to increased oil formation. The amount of solid residue remained nearly constant when the temperature increased from 400 °C to 450 °C, indicating that char formation stabilised at around 400 °C. It is also noteworthy that the formation of WSP occurred

during the HTL of SD at 350 °C and 400 °C, which decreased as temperature increased. WSPs are mainly composed of intermediate compounds, which would eventually repolymerise to form oil or char with increasing process severity (Fan et al., 2022). Hence, no measurable WSP was obtained from SD at 450 °C. The yield of oil from SD decreased by 4% when the temperature was increased from 400 °C to 450 °C, while gas yield increased by 17%, which may indicate the possible reaction of oil components with hot-pressurised water medium.

For the plastic feedstocks, no substantial degradation was observed up to 400 °C. At 350 °C and 400 °C, the experiment with LDPE produced mostly melted plastics, with only 2.05 wt% and 5.16 wt% of oils, respectively. Similarly, HDPE produced 2.55 wt% and 6.51 wt% of oils at 350 °C and 400 °C, respectively. Hence, up to 400 °C, the solid residues recovered from the plastics were unconverted plastics rather than char (product of carbonisation). These melted plastics accounted for

Table 2

Product yields and mass balances from non-catalytic hydrothermal conversion of individual feedstocks in relation to temperature after 1 h reaction time.

Sample	Temperature (°C)	Pressure (bar)	Gas (wt%)	Oil (wt%)	Solid residue (wt%)	WSP (wt%)	Balance (wt%)
SD	350	20.7	11.6	15.5	69.4	2.05	98.6
SD	400	25.7	13.5	42.2	40.8	1.12	97.6
SD	450	28.1	15.8	40.5	40.1	–	96.4
LDPE	350	18.7	0.56	2.05	95.5	–	98.1
LDPE	400	20.1	1.66	5.16	92.1	–	98.9
LDPE	450	25.7	3.02	81.3	14.7	–	99.0
HDPE	350	19.3	0.21	2.55	95.7	–	98.5
HDPE	400	21.3	0.85	6.51	90.3	–	97.7
HDPE	450	26.1	2.12	88.1	5.86	–	96.1

>90 wt% of the feed used. This agreed with the work reported by Sebestyén et al. (2022) that HTL of PP at 350 °C without a catalyst produced 83 wt% solid. At 450 °C, there was a dramatic increase in the yields of oils from the plastics, as the temperature provided the energy required from their degradation. In addition, thermal degradation of plastics is known to occur at much higher temperatures than biomass (Jin et al., 2021; Mukundan et al., 2022; Laredo et al., 2023). For instance, Sebestyén et al. (2022) obtained 91 wt% of oil products, comprising of 80% naphtha range compounds was obtained when they increased HTL temperature to 425 °C.

Results in Table 2 shows that for the plastics, the main reaction that occurred during experiments at 450 °C was the conversion to oil of the melted plastics that were observed at lower temperatures. Hence, at 450 °C, oil products dominated the HTL of the plastics, accounting for more than 81 wt% of the feedstock used, similar to the work of Jin et al. (2021). For LDPE, the amount of solid residue decreased to 14.7 wt%, while for HDPE a further decrease of solid residue to 5.86 wt% was obtained. HDPE produced more oil than LDPE in these experiments, probably because the presence of branched chains in the LDPE structure tend to undergo secondary condensation reactions to form char (Sogancioglu et al., 2017). Moreover, the solid residues from the HTL of the plastics were black friable materials, indicating these were char products rather than melted plastics. Clearly, the results from the plastics showed that higher temperatures were required for their degradation under the hydrothermal conditions used in this study (Jin et al., 2021). Additionally, there were marginal increases in the yields of gas products from these plastics, which mostly contained C₁–C₄ hydrocarbon gases, like those reported in literature during the HTL polyolefin plastics (Colnik et al., 2022; Mukundan et al., 2022).

In this present work therefore, the total conversions of all three individual feedstocks only occurred at 450 °C, making it the appropriate temperature to compare their product yields. At 450 °C, HTL of SD alone produced much higher yields of solid residue (40.1 wt%) than the LDPE (14.7 wt%) and HDPE (5.86 wt%). This was not unexpected considering that the SD sample already contained a total of 16.4 wt% of solid-borne ash and fixed carbon (Table 1). In addition, char formation during thermochemical conversion of biomass is well known to occur via dehydration of holocellulose fractions (Minowa and Ogi, 1998; Williams and Onwudili, 2006; Seshasayee and Savage, 2021) and the degradation of lignin, followed by subsequent condensation of phenolic compounds (Jahirul et al., 2012).

3.2. Influence of temperature on product yields from catalytic HTL of individual feedstocks

Table 3 presents the product yields and mass balances (≥ 95 wt%) from the HTL of the individual feedstocks in the presence of the Ni–Cu/Al₂O₃ catalyst at different temperatures for 1 h reaction time. The general trends in the yields of products from these catalytic experiments were like those obtained from the non-catalytic tests. However, the results show that the presence of the catalyst increased gas and oil formation from SD compared to the non-catalytic tests. Indeed, oil yield of

38.1 wt% from SD was obtained at 350 °C in the presence of the catalyst, which was 2.5 times higher than the yield from the corresponding non-catalytic test (Table 2). Increasing the reaction temperature to 400 °C, led to an increase in SD oil yield by 27%–48.5 wt%. Further increase in temperature to 450 °C, did not seem to alter the oil yield (48.2 wt%). The increases in SD gas and oil yields with increasing temperature from 350 °C to 400 °C, corresponded to decreasing amounts of solid residues. However, between 400 °C and 450 °C, the most noticeable change was the increase in gas yield from SD, which may be attributed to the increased catalysed reactivity of the hot-pressurised water probably with char.

In contrast to SD, the presence of the catalyst caused appreciable decreases in the oil yields from the two plastic feedstocks, when compared to the non-catalytic tests. These results indicated that the catalyst promoted the conversion of the liquid products to gas and char, with the liquid-to-gas conversion being more dominant (Cheng et al., 2017). For the individual plastic feedstocks, the lower oil yields appeared to correspond to increased gas yields for LDPE and increased char yields for HDPE. Comparing the two plastics, HDPE produced more oil but less gas and char than LDPE when reacted in the presence of Ni–Cu/Al₂O₃ at 450 °C. The increased char yield could have affected the compositions of the oil products as discussed in Section 3.5.

3.3. Influence of temperature on product yields from non-catalytic co-HTL of mixed feedstocks

Following the results of the influence of temperature on the yields of products from the non-catalytic HTL of individual feedstocks, experiments were designed to investigate the co-HTL of the mixed feedstocks (SD/LDPE and SD/HDPE) under similar temperature conditions. In this case, 2 g of mixed feedstocks comprising 1 g of SD and 1 g of LDPE or HDPE were used in each experiment. The results are presented in Table 4, with mass balances greater than 96 wt%. Like results from individual feedstocks, the processing of the mixed feedstocks at 350 °C and 400 °C, produced WSPs essentially from the SD component but none was observed at 450 °C. Due to its weaker covalent structure, the SD component in the feed was able to undergo degradation to produce oil, gas and char even at 350 °C, whereas the plastics could only completely degrade at 450 °C in this study (Table 2). Hence, oil yields from the mixed feedstocks were found to increase with increasing temperature due to increased conversion of the plastics. The SD/HDPE mixtures produced more oils and less gas than the SD/LDPE mixtures across all three temperatures (Sogancioglu et al., 2017).

The evaluation of synergistic interactions during the formation of reaction productions from non-catalytic co-HTL of SD and the plastics was carried out by the applying data in Tables 2 and 4 in Equations (8) and (9), respectively. The values of synergy factors in Fig. 1 show that there were minor interactions between SD and each plastic feedstock during reactions at 350 °C and 400 °C.

At 350 °C, the presence of the plastics (melted) appeared to similarly reduce gas and char formation compared to the individual feedstocks. Then at 400 °C, the mixtures behaved differently. SD/LDPE gave

Table 3
Product yields and mass balances from catalytic hydrothermal conversion of individual feedstocks in relation to temperature after 1 h reaction time.

Sample	Temperature (°C)	Pressure (bar)	Gas (wt%)	Oil (wt%)	Solid residue (wt%)	WSP (wt%)	Balance (wt%)
SD	350	21.8	13.5	38.1	44.5	2.16	98.3
SD	400	26.3	17.6	48.5	31.1	1.27	98.5
SD	450	28.3	20.2	48.2	28.6	–	97.0
LDPE	350	19.1	0.78	2.24	95.3	–	98.3
LDPE	400	20.5	2.75	6.23	89.6	–	98.6
LDPE	450	26.1	8.26	76.6	12.1	–	97.0
HDPE	350	20.0	0.23	4.11	93.7	–	98.0
HDPE	400	22.7	1.38	8.66	86.2	–	96.2
HDPE	450	26.3	5.23	79.1	10.7	–	95.0

Table 4

Product yields and mass balances from non-catalytic co-HTL of mixed SD and plastic feedstocks in relation to temperature after 1 h reaction time.

Sample	Temperature (°C)	Pressure (bar)	Gas (wt%)	Oil (wt%)	Solid residue (wt%)	WSP (wt%)	Balance (wt%)
SD/LDPE	350	18.5	5.85	8.75	81.1	1.85	97.6
SD/HDPE	350	18.2	5.01	9.26	79.6	1.91	95.8
SD/LDPE	400	20.5	8.13	20.7	68.1	0.32	97.3
SD/HDPE	400	20.8	6.76	23.5	65.6	0.36	96.2
SD/LDPE	450	26.1	11.6	66.8	18.2	–	96.6
SD/HDPE	450	26.8	9.44	71.2	16.5	–	97.1

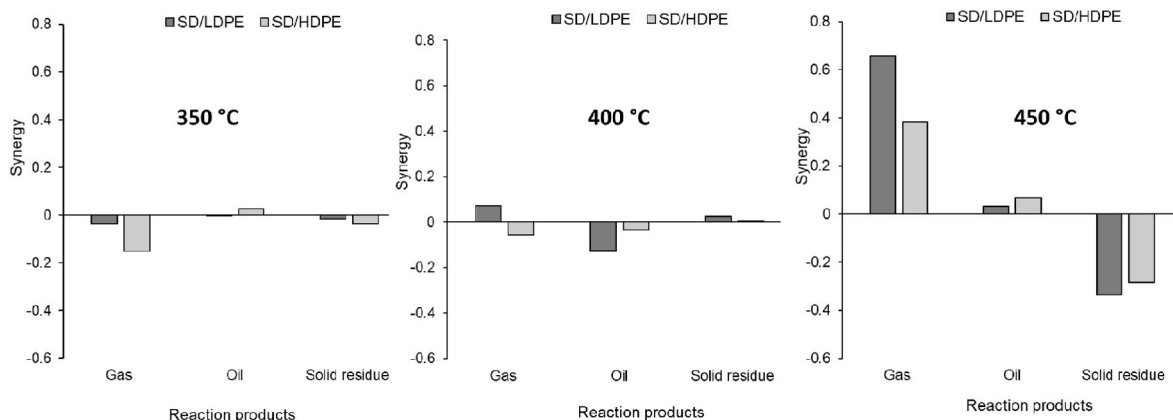


Fig. 1. Synergy factors indicating the extent of interactions between SD and plastic feedstocks on product yields during non-catalytic co-HTL at different temperatures.

Table 5

Product yields and mass balances from catalytic co-HTL of mixed SD and plastic feedstocks in relation to temperature after 1 h reaction time.

Sample	Temperature (°C)	Pressure (bar)	Gas (wt%)	Oil (wt%)	Solid residue (wt%)	WSP (wt%)	Balance (wt%)
SD/LDPE	350	20.2	6.95	20.5	69.7	1.67	98.8
SD/HDPE	350	20.5	7.87	21.6	66.6	1.24	97.3
SD/LDPE	400	23.6	12.1	23.8	62.5	0.18	98.6
SD/HDPE	400	23.8	10.5	25.6	60.2	0.16	96.5
SD/LDPE	450	27.6	16.8	64.1	15.7	–	96.6
SD/HDPE	450	27.4	16.3	66.7	12.6	–	95.6

negative synergy for oil formation while gas and char yields were enhanced. For SD/HDPE, negative synergy was observed for gas and oil yields while char remained unchanged. As shown in Fig. 1, the interactions between the intermediate products from the co-HTL of SD and the plastics lead to enhancement of gas and oil yields at 450 °C in both cases (Mukundan et al., 2022; Laredo et al., 2023). The mixed feedstocks (SD/LDPE and SD/HDPE) gave positive synergy factors for oil and gas production. Consequently, the yields of solid residues decreased

substantially in favour of gas products much more than the oils. The results in Fig. 1 show that SD/LDPE feedstock favoured more gas production, whereas SD/HDPE slightly favoured more oil production, both by lowering the amount of solid residues. The reason for these trends could be linked to the presence of reactive intermediates which prevented char-forming reactions such as aromatisation and aromatic condensation from the SD. Plastic degradation is known to proceed via the generation of large amounts of radical species, which may interact

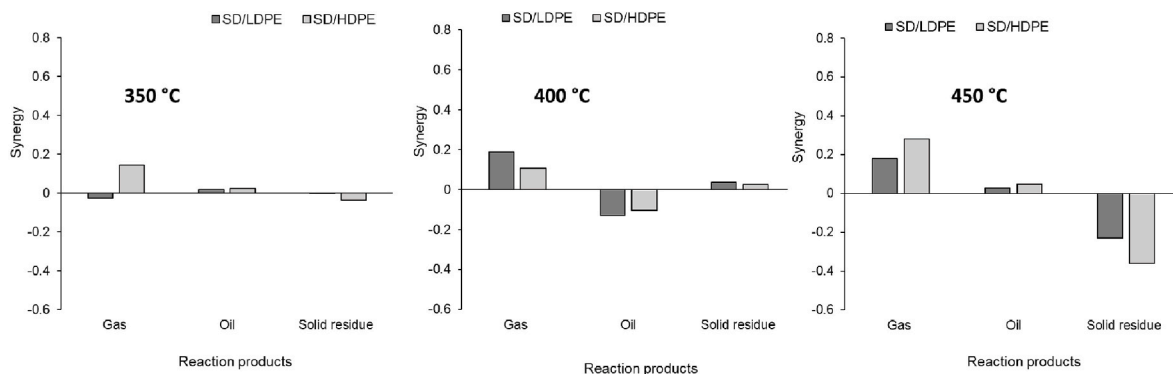


Fig. 2. Synergy factors indicating the extent of interactions between SD and plastic feedstocks on product yield during catalytic co-HTL with Ni-Cu/Al₂O₃ at different temperatures.

with SD intermediates to prevent their stabilisation into char.

3.4. Influence of temperature on product yields from catalytic co-HTL of mixed feedstocks

The influence of Ni-Cu/Al₂O₃ catalysts during the co-HTL of the mixed SD/LDPE and SD/HDPE feedstocks was further investigated in relation to reaction temperatures (350 °C–450 °C). The results are presented in Table 5. Like the non-catalytic tests, the Ni-Cu/Al₂O₃ catalyst did not seem to promote the degradation of the plastics for reactions up to 400 °C. Hence, the yields of oils and gas remained low, while solid residues (melted plastics) were the main products at 350 °C and 400 °C. Indeed, the solid residues from the SD/LDPE experiments at 400 °C still contained whitish plastic material, whereas the solid residue from SD/HDPE was completely blackened at the same temperature.

The main differences between the catalytic and non-catalytic tests can be seen in the enhanced yields of gas and oil products. For example, at 350 °C the oil yield from the catalytic test was more than double the yield without the catalyst at the same temperature for both SD/LDPE and SD/HDPE. However, there was only marginal increases at 400 °C due to the resistance of the plastics to degradation. Hence, most of the oil products from the experiments with the mixed feedstocks up to 400 °C came from SD, with little contributions from the plastics. Then, with a further increase in temperature to 450 °C, the oil products increased to above 60 wt%, like the case of the non-catalytic tests. This indicated that both the SD and plastics contributed to oil (and gas formation) at 450 °C, mostly due to the effect of high temperature. Instead, the use of the catalyst led to decreased oil yields compared to the non-catalytic tests. Although, high oil yields are desirable, the compositions of the oils are equally of utmost importance for their eventual use e.g., as liquid fuel or fuel additives. This can be especially true if the observed loss is due to removal of oxygen atoms in the SD-derived bio-oils via deoxygenation

reactions to produce hydrocarbon-rich liquids as shown by GC/MS analysis results in Section 3.5.

The plot of the synergy factors from these experiments are shown in Fig. 2 to underline the influence of the catalyst. The mixed feedstocks behaved differently in the presence of the catalyst at 350 °C but gas similar synergy profiles at 400 °C and 450 °C, respectively. At 350 °C, slightly positive synergies were observed for oil production from both feedstocks. However, SD/HDPE gave positive synergy for gas formation and slightly negative synergy for char formation, while for SD/LDPE, gas formation was reduced while char formation barely changed. At 400 °C, the interactions between SD and the plastics promoted both gas and char formation, with negative synergies for oil production. The melting of the plastics could have prevented the SD from degrading into oil products, as was the case with SD alone at this temperature. At 450 °C, large positive synergies for gas production and negative synergies for char formation were equally observed for both SD/LDPE and SD/HDPE. Both feedstocks showed slightly positive synergies for oil formation. Overall, the reaction at 450 °C, showed that interactions between the degradation products of SD and the plastics promoted gas formation in favour of solid residues or char formation, due to the conversion of the plastics.

3.5. Compositions of oil products from HTL and co-HTL studies at 450 °C

The results above show that complete conversion of all three solid feedstocks only occurred at 450 °C. Therefore, the aim of this research for co-HTL of the biomass and plastics to produce hydrocarbon-rich oil was only realised at this temperature. However, giving the similarity in products yields between the two sets of non-catalytic and catalytic experiments, the effect of the catalyst did not seem obvious. Hence, the results of the GC/MS analyses of the oil products obtained only at 450 °C for both individual and mixed feedstocks are reported here.

3.5.1. Compositions of oil products from HTL of individual feedstocks at 450 °C

The detailed composition of the oil products from the non-catalytic and catalytic HTL of SD, LDPE and HDPE, respectively, are presented as peak area percent (%) in Fig. 3. The DCM-soluble oil product from the non-catalytic HTL of sawdust contained 93.6% oxygenated compounds, dominated by ketones (49.6%), phenolic compounds (22.4%), furfural (16.7%), which are typical of HTL bio-oils (Ansari et al., 2019). Small yields of furans (2.58%) and carboxylic acids (2.37%) were also obtained from SD. The oil product from SD did not contain any aromatic hydrocarbons in the absence of the catalyst. For LDPE and HDPE, which are purely hydrocarbon polymers, their non-catalytic HTL oil products were mainly composed of alkanes and alkenes, with combined peak areas of >97% in each case. The HTL of LDPE produced more alkanes (55.2%) and less alkenes (42.6%) than HDPE (49.6% alkanes and 50.4% alkenes). Table 6 shows that the carbon content in the SD bio-oil increased by 16.3%, while the oxygen content decreased by 22% in the presence of the catalyst, compared to the non-catalytic tests. Hence, the HHV of the bio-oil increased by 25% with the use of the catalyst. For

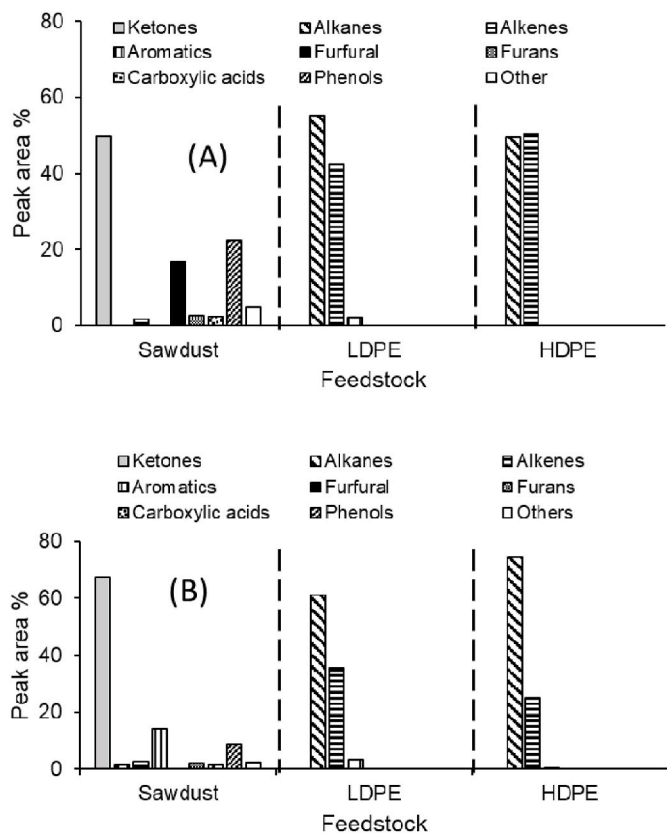


Fig. 3. Compositions of oil products from the HTL of individual feedstocks at 450 °C for 1 h (A) without catalyst; (B) with Ni-Cu/Al₂O₃ catalyst.

Table 6
Elemental compositions and HHV of oil products from the non-catalytic and catalytic HTL of individual feedstocks at 450 °C, 1 h reaction time.

Sample	C (wt %)	H (wt %)	N (wt %)	S (wt %)	O (wt %)	HHV (MJ/kg)
SD	50.9	6.43	0.23	0	42.7	19.8
SD + Ni-Cu/Al ₂ O ₃	59.2	7.09	0.21	0	33.5	24.8
LDPE	85.3	14.5	0.17	0	0.03	48.7
LDPE + Ni-Cu/Al ₂ O ₃	85.6	14.2	0.19	0	0.01	48.3
HDPE	85.1	14.7	0.23	0	0.01	48.8
HDPE + Ni-Cu/Al ₂ O ₃	85.4	14.4	0.16	0	0.01	48.5

LDPE and HDPE, Table 6 shows no significant changes in the elemental compositions and HHVs of their oil products, which were entirely hydrocarbons as shown in Fig. 3.

In the absence of the catalyst, the oil product from LDPE contained ≈2% aromatic compounds, whereas none was observed in the oil from HDPE. Dry pyrolysis of LDPE has been reported to produce oils with much higher contents of aromatic compounds than HDPE (Sogancioglu et al., 2017). It would seem from this present work, that HTL did not favour aromatic production from the plastics, particularly LDPE, compared to pyrolysis. As shown in Fig. 3a, no oxygenated compounds were formed from the non-catalytic HTL of the plastic feedstocks. This indicated that there were no significant chemical interactions between the water medium and the plastics and their intermediate degradation products to form oxygenates. Previous research reported that the presence of molecular oxygen or strong oxidizing agents like hydrogen peroxide was required to produce oxygenated from hydrocarbon feedstocks under hydrothermal conditions (Onwudili and Williams, 2007). This is advantageous for HTL of polyolefin plastics to produce pure hydrocarbons in water reaction media (Jin et al., 2021).

In the presence of the Ni-Cu/Al₂O₃ catalyst, the composition of the oil products changed dramatically for all three feedstocks. For the sawdust, the dominance of ketones became more pronounced with 70.6% of total peak areas compared to value of nearly 50% without the catalyst. Interestingly, complete conversion of furfural was observed for sawdust in the presence of the catalyst; instead, 14.2% of aromatic hydrocarbons (toluene, ethylbenzene, styrene and 1,3-dephenylbenzene) was produced. The formation of aromatic hydrocarbons via Diels-Alder cycloaddition of furans and alkenes have been well reported in literature (Green et al., 2016). Hence, the disappearance of furfural and formation of aromatic hydrocarbon may indicate the activity of this bimetallic catalyst for this type of reaction. The oil products from the individual HTL of LDPE and HDPE were composed entirely of hydrocarbons from C₇ to C₃₃. In addition, the catalyst seemed to have enhanced the yields of alkanes to the detriment of alkenes. The combined peak areas of alkanes in the oils from the HTL of LDPE was 61.03% compared to 55.2% without the catalyst, while the combined peak areas of alkenes decreased from 42.6% to 35.7%. Similarly for HDPE, there was an even larger shift towards alkanes compare to LDPE, with 72.4% combined peak areas for alkanes, while those of alkenes decreased by half from 50.4% to 25.1%. The increased alkanes contents in the oils in the presence of the catalyst could possibly be via hydrogenation by in-situ generated hydrogen (Fu et al., 2011).

Fig. 4 shows the carbon number distribution of alkanes and alkenes in the oils obtained from the non-catalytic and catalytic tests, which may

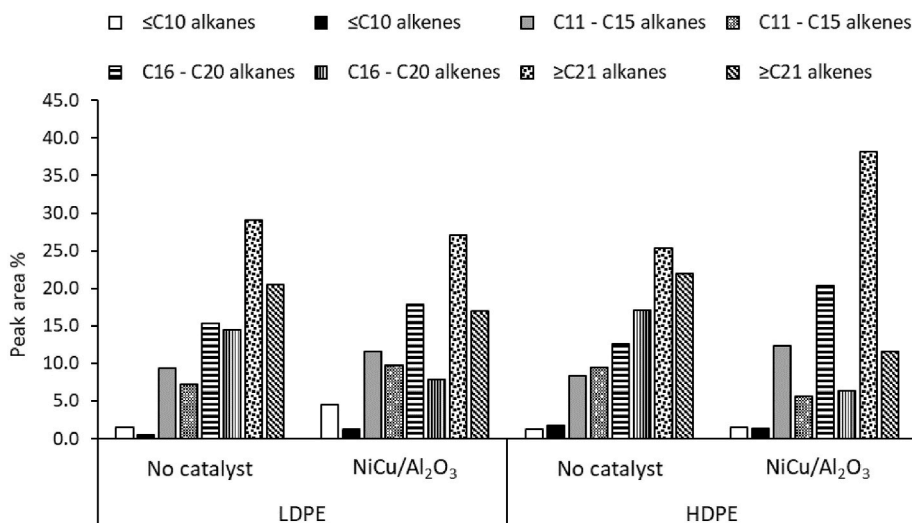


Fig. 4. Distribution of hydrocarbons in the oil products obtained from the individual HTL of LDPE and HDPE at 450 °C for 1 h.

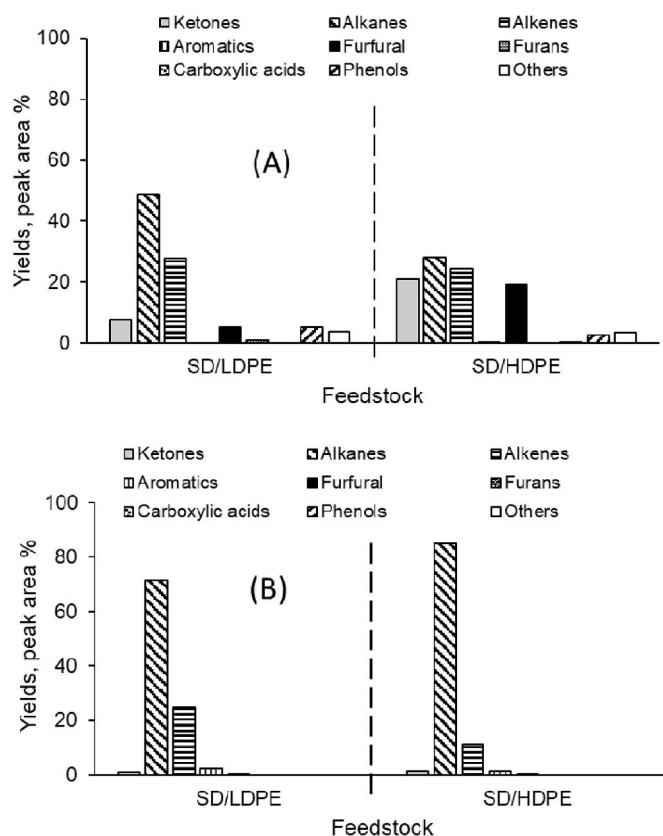


Fig. 5. Compositions of oil products from the co-HTL of sawdust with the plastic feedstocks at 450 °C for 1 h; (A) without catalyst; (B) with Ni-Cu/Al₂O₃ catalyst.

support the *in-situ* dehydrogenation and hydrogenation mechanisms. The results presented in Fig. 4, shows that for LDPE, the main increase of alkanes occurred within the C₁₆-C₂₀ range, whereas for HDPE, the formation of alkanes also increased for the C₁₆-C₂₀ range, but significantly for the ≥C₂₁ compounds.

3.5.2. Compositions of oil (liquid) products from co-HTL of SD/LDPE and SD/HDPE at 450 °C

Fig. 5 shows the compositions of liquid products obtained from co-HTL of sawdust and the plastics, with and without the Ni-Cu/Al₂O₃

Table 7

Elemental compositions and HHV of oil products from the non-catalytic and catalytic co-HTL of mixed feedstocks at 450 °C, 1 h reaction time.

Sample	C (wt %)	H (wt %)	N (wt %)	S (wt %)	O (wt %)	HHV (MJ/kg)
SD/LDPE	63.4	9.08	0.22	0	27.3	29.9
SD/LDPE + Ni-Cu/Al ₂ O ₃	81.9	14.1	0.18	0	3.82	46.4
SD/HDPE	61.8	10.4	0.18	0	27.5	31.1
SD/HDPE + Ni-Cu/Al ₂ O ₃	82.3	14.3	0.18	0	3.22	46.9

catalyst at 450 °C. Fig. 5a shows the distribution of different classes of organic compounds obtained from the non-catalytic co-HTL of sawdust and the polyolefin plastics.

The results showed that while alkanes and alkenes dominated the oils (arising mostly from the plastics), other biomass-based products such as ketones, furfural, carboxylic acids, and phenols were also present. Hence, the conversion of these oxygenated compounds was not very effective without the catalyst. Indeed, in terms of peak area %, SD/HDPE produced much higher yields of ketones (21%) and furfural (19.2%) than SD/LDPE, which produced 7.87% and 5.04% of these compounds, respectively. These may indicate higher levels of interactions between the degradation products of SD and LDPE than SD and HDPE, leading to the conversion of the oxygenates during their respective co-HTL tests. The reduced yields of oxygenates from SD/DPE may therefore be linked to their conversion to gas and char according to Table 3. In addition, the oils from the non-catalytic co-HTL of the mixed feedstocks did not contain any aromatic hydrocarbons.

In the presence of Ni-Cu/Al₂O₃ catalyst, it was observed that, apart from furfural with yields of <0.5%, no other oxygenated compounds were observed in the oil products from the catalysed co-HTL experiments. Instead, Fig. 5b shows that the oil products were dominated largely by alkanes followed by alkenes. The yield of aromatics from both co-HTL experiments remained low at below 3% in each case, with 2.31% and 2.24% from SD/LDPE and SD/HDPE, respectively. These results indicated that the presence of the plastic degradation products promoted the conversion of sawdust into hydrocarbon-rich oils as shown in Fig. 5b.

In addition, the interactions of the degradation products of SD and the plastics led to improved deoxygenation as shown in the elemental analysis data provide in Table 7. Without the catalyst, both SD/LDPE and SD/HDPE produced liquids with HHV of around 30 MJ/kg, which was much higher than that of the oil with SD alone but much lower than the oils from the individual plastics. However, in the presence of Ni-Cu/Al₂O₃, the HHV of the resulting oils increased to within the range of conventional diesel and kerosene fuels. The degree of catalytic deoxygenation in the oils are apparent in Table 7, where oxygen contents decreased by 86% for SD/LDPE between the catalytic and non-catalytic co-HTL tests. For SD/HDPE, the degree of catalytic deoxygenation was

slightly higher at 88.3%.

Hence, the interactions between the degradation products of SD and the plastics may have significantly influenced the compositions of the resulting oil products. Interestingly, the oil products from the co-HTL tests contained a range of cycloalkanes and alkyl cycloalkanes that were not observed in the oils from the individual plastics. These compounds accounted for 2.43% and 8.6% of peak areas in the oils from co-HTL of SD/LDPE and SD/HDPE, respectively. For the oil from co-HTL SD/HDPE, these compounds included short-chain cycloalkanes with long-chain alkyl groups such as hexyl cyclopropane to long-chain cycloalkanes up to C₂₃ (e.g., cyclotricosane). In contrast, the oil from SD/LDPE contained cycloalkanes up to C₁₅ (e.g., cyclopentadecane). One possible explanation for the presence of these compounds would be their formation via end-chain cyclisation of alpha-olefins produced from the plastics. This could be a plausible explanation since the oils from co-HTL contained higher contents of these cycloalkanes and lower contents of alkenes than those from the individual plastics.

As shown in Fig. 6, the possibility of synergistic interactions between the degradation products of SD and the plastics is supported by the dramatic disappearance of furfural in oils from SD/LDPE and SD/HDPE, with or without catalysts. Furthermore, without the catalyst, the interactions also led to reduction or complete disappearance of aromatic compounds. Fig. 7 provides plausible reaction pathways for the changes in the range of compounds found in the oils obtained especially from the catalytic co-HTL experiments. Giving the SD and plastics degraded under different temperature ranges, it would appear that interactions between the feedstocks were not as important for oil formation and composition. Instead, after the initial thermal degradation of the feedstocks, interactions between their degradation products must have influenced the yields and compositions of the oil products. Reactions within and between intermediates such as Diels-Alder addition/cycloaddition between alkenes from plastics and furfural from SD, followed by hydrogenation would lead to mid-range cycloalkanes. Also, aldol condensation between SD-derived bio-oils would produce longer change ketones, which could be hydrogenated to fuel range liquid alkanes. For the plastics, the possible catalytic generation of *in situ* hydrogen would have provided the right reaction environment for hydrogenation of alkenes to alkanes as well as the hydrogenolytic C-C bond cleavages to produce mid-range alkanes.

3.5.3. Effect of reaction time on non-catalytic and catalytic co-HTL of SD/LDPE at 450 °C

Overall, the reaction at 450 °C for 1 h was most successful in converting all three feedstocks into gas and oil products with or without the Ni-Cu/Al₂O₃ catalyst. In this section, the influence of reaction time was carried out at 450 °C for reaction times ranging from 0.5 to 4 h, to investigate how reaction products and their compositions could change to give better results than those obtained from 1 h of reaction. Fig. 8 presents the product yields and mass balances from these catalytic and

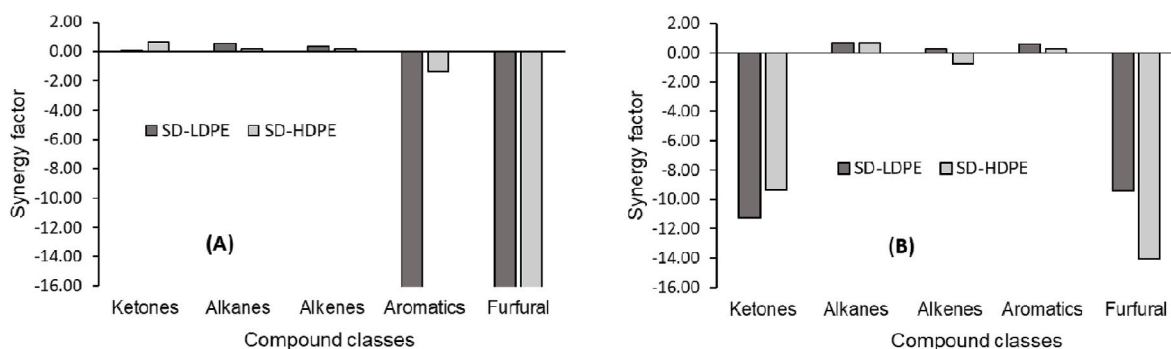


Fig. 6. Synergy factors indicating possible interactions for key oil components formation during co-HTL of SD/LDPE and SD/HDPE; (A) without catalyst and (B) with Ni-Cu/Al₂O₃ at 450 °C.

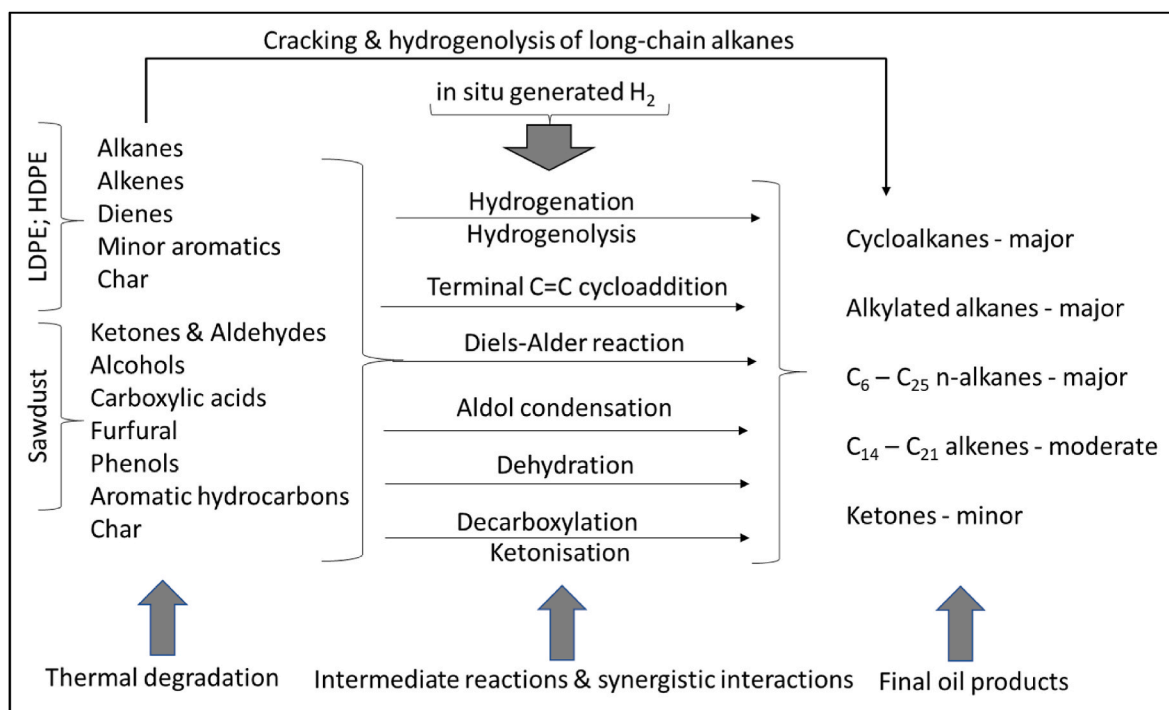


Fig. 7. Plausible reaction pathways leading to the formation of final oil products.

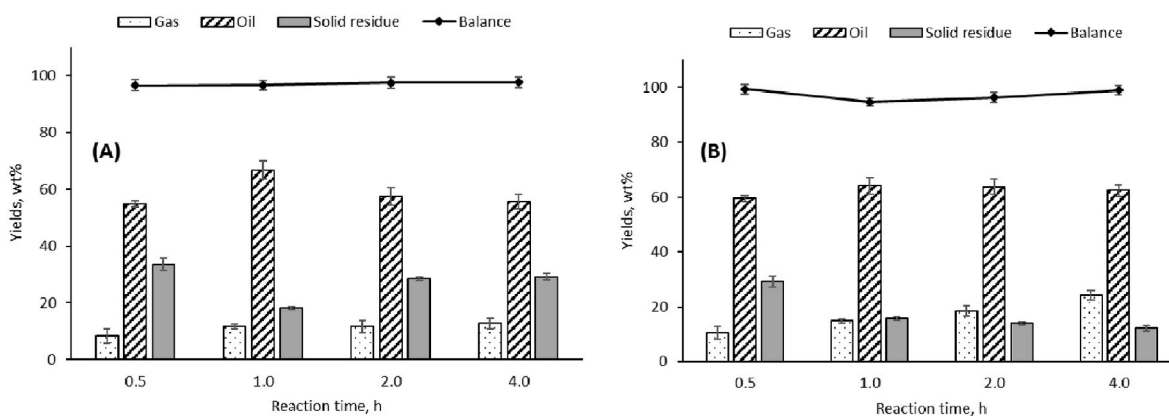


Fig. 8. Effect of reaction times of product yields and mass balances during co-HTL of SD/LDPE at 450 °C; (A) without catalyst (B) with Ni-Cu/Al₂O₃.

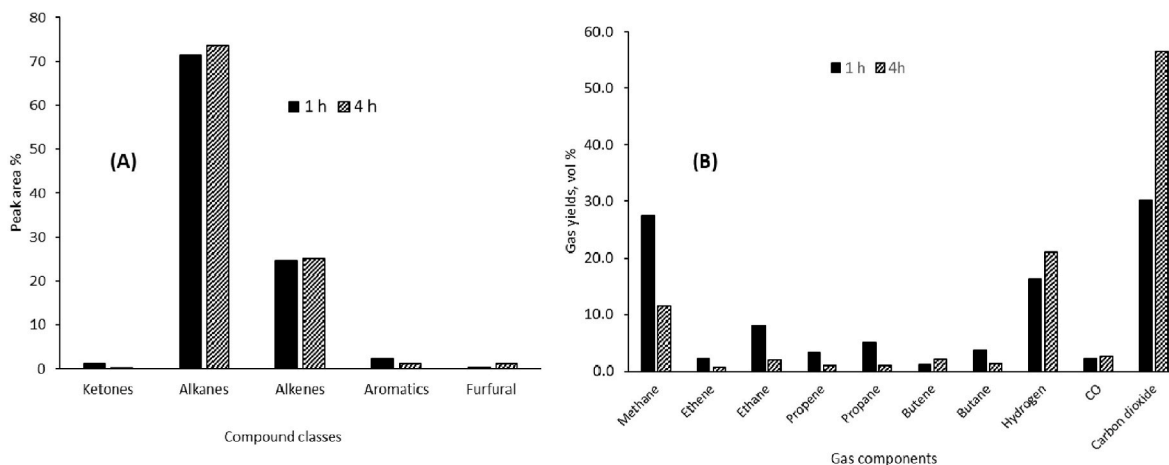


Fig. 9. Compositions of oil products (A) and compositions of gas products (B) from co-HTL of SD/LDPE at 450 °C for 1 h and 4 h.

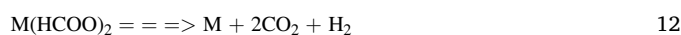
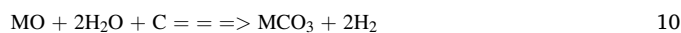
non-catalytic experiments.

The results showed that high conversion rates of the mixed feedstock to liquid products were achieved even after 0.5 h of reaction at 450 °C, with and without the catalyst. The general trend observed from non-catalytic experiments was that the yields of oil and gas product increased between 0.5 and 1 h reaction times, then oil yields decreased, while gas and char yields increased with increased reaction time. In the absence of the catalyst, the extended reaction time promoted secondary reactions that led to char and gas formation from the oil products. Studies have shown that during HTL, increased reaction severity (i.e., increasing temperature and reaction time) would promote the cracking of compounds in the oil products into gas components (Wagner et al., 2016; Watson et al., 2020). In the presence of the catalyst, gas formation increased much more compared to the non-catalytic tests as reaction time increased. The presence of the catalyst led to increased gas formation and reduced yields of oil and char in relation to increasing reaction time.

The trends in the yields of solid residues indicate that the conversions of the plastics in the mixed feedstocks were incomplete after 0.5 h, with and without the catalyst. However, the lower yield of solid residues in the presence of the catalyst indicated that it promoted higher solid conversion during the first 0.5 h compared to the results of the corresponding non-catalytic test. Interestingly, the Ni-Cu/Al₂O₃ continued to enhance solid conversion with time, which may explain some of its catalytic activities. For instance, the continued reduction solid residues and the increase in gas yields indicated that the catalyst could convert solid residues into gas through redox catalysis. Hence, the compositions of the gas and oil products obtained in the presence of the catalyst at 450 °C at 1 h and 4 h reaction times, were respectively analysed and presented in Fig. 9. Interestingly, Fig. 9A shows that no significant changes occurred in the compositions of the oil products between the catalytic reactions at 1 h and 4 h.

In addition, results in Fig. 9B shows that the gas product obtained after 1h was dominated by hydrocarbon gases with 51.1 vol%, while hydrogen and carbon dioxide were 16.4 vol% and 30.2 vol%, respectively. After 4 h of reaction at the same temperature, the total yield of hydrocarbon gases fell to 19.7 vol%, while hydrogen and carbon dioxide increased to 21.0 vol% and 56.6 vol%, respectively. The increased formation of hydrogen gas, and especially carbon dioxide, may support a

possible redox catalysis of Ni-Cu/Al₂O₃. Although, the presence of the catalyst promoted char formation from the plastics (Table 3), it was unlikely that the char-forming reactions would produce sufficient hydrogen to account for the increased yields of alkanes, especially for HDPE. Therefore, the additional hydrogen to facilitate hydrogenation of alkenes could come from the water medium used for the reaction. For instance, the preferential formation of alkanes over alkenes during catalytic hydrothermal processing of unsaturated long-chain compounds (e.g., oleic acid) has been reported without external hydrogen addition by several authors [Fu et al., (2011)]. This has been linked to *in-situ* formation of hydrogen via metal carbonate-metal formate intermediates in the presence of CO₂ in hydrothermal media (Onsager, et al., 1996; Kruse and Dinjus, 2005; Yao et al., 2017). However, the HTL of polyolefin plastics hardly produces high concentrations of CO₂, so that the mechanism may involve the carbon atoms from the carbon-rich polymer framework of the plastics or from the char produced during the reaction. For instance, in the presence of transition metal-based catalysts, the following catalytic redox reactions could occur between metals, carbon and water (Equations 10–13):



Essentially, the overall reaction depicts the catalysed reaction of water with carbon (water-gas reaction) in Equation (14):



The production of hydrogen could explain the increased hydrogenation of the oils in the presence of the catalyst, leading, initially to increase in the yields of alkanes in the oil products. The possible continued *in situ* generation of hydrogen also helped to maintain high alkane contents in the oils even after 4 h. Other researchers have reported that increased reaction severity led to increased aromatic formation during thermal processing of plastics (Muhammad et al., 2015), but this was not observed in this present work with the Ni-Cu/Al₂O₃ catalyst.

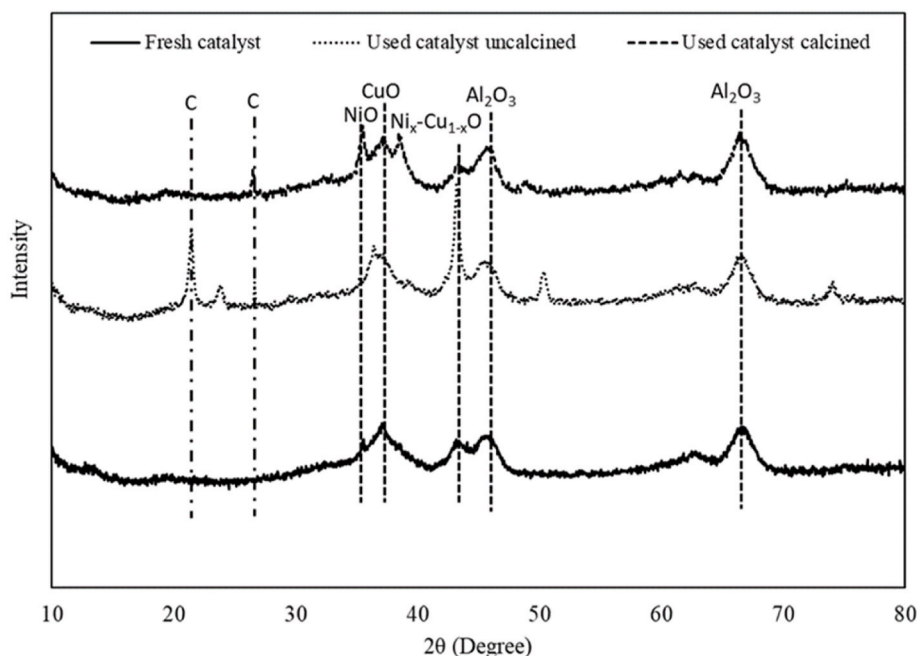


Fig. 10. XRD patterns of fresh, used uncalcined and used calcined Ni-Cu/Al₂O₃ catalyst.

Hence, the results from this present study indicated that extending the reaction time from 1 h to 4 h, mainly favoured gas production from the conversion of the solid residues rather than the oils. In the presence of the Ni–Cu/Al₂O₃ catalyst, oil yields only changed slightly, with values between 60 wt% and 64 wt%. Therefore, the co-HTL of SD/LDPE, and by extension, SD/HDPE could be successfully carried out at 450 °C for 1 h or less. This makes the process potentially viable for valorising the large quantities of plastics and biomass into hydrocarbon-rich liquids dominated by alkanes, and therefore suitable for use as fuels.

3.6. Regeneration of used Ni–Cu/Al₂O₃ catalyst

The recovered solid residue from the catalytic experiments contained the used catalysts and any solid residues (char at 450 °C). The catalysts were recovered by calcination in a muffle furnace at 550 °C for 2 h, which led to burn-off of carbonaceous materials. The phase compositions of the fresh and recovered catalyst samples were determined using X-ray powder diffraction using a Bruker D8 X-ray diffractometer with a Cu K α X-ray source operating at 40 kV and 40 mA and a Vantec position sensitive detector. The diffraction angle 2 theta between the detector and X-ray source was varied from 10 to 80° at a scanning speed of 0.05°/s. The spectra were analysed with a database of known spectra to identify the peaks using High Score Plus software. An extensive characterisation of the fresh and used Ni–Cu/Al₂O₃ catalyst has been carried out in a recent publication, which showed that it was stable under hydrothermal conditions (Alves and Onwudili, 2022).

The XRD spectrograms are presented in Fig. 10, which shows the presence of carbon deposits on the used catalyst before calcination at 2 θ = 22° and 43.4°, where it overlapped at the latter with the Ni_x–Cu_{1-x}O peak. The diffraction peaks at 2 θ = 37.3°, 45.8° and 67.3° corresponded to the crystalline phase of γ -Al₂O₃, the catalyst support material. Overall, the catalyst appeared to be restored to nearly its fresh original form after calcination. Further tests on the reusability of the recovered catalyst will be carried out as part of future process optimisation, but regeneration by calcination appeared to be promising.

4. Conclusions

In this present study, low-pressure (<30 bar) non-catalytic and catalytic co-HTL of biomass (sawdust) and polyolefin plastics (LDPE and HDPE) have been investigated with a focus on the oil products. The reaction temperature of 450 °C led to complete conversion of plastics in 1 h reaction time and, therefore provided the optimum conditions for the co-HTL tests. The results showed evidence of synergistic interactions of the degradation products of the biomass and plastic feedstocks leading to the production of highly deoxygenated oils dominated by fuel-range alkanes. The presence of the plastic degradation products prevented the extensive carbonisation of the biomass often associated hydrothermal conversion processes. In addition, the catalytic reaction environment seemed to generate *in situ* hydrogen, which provided hydrogenation capacity even for longer reaction times of up to 4 h, to maintain the high yields of alkanes in the related oil products. In comparison with the non-catalytic tests, the Ni–Cu/Al₂O₃ catalyst was highly efficient in the deoxygenation of the oil obtained from the mixed feedstocks, leading to improved hydrocarbon yields and therefore, higher fuel quality. Results from this present work have shown that using this single novel low-pressure process loop has the potential to reduce engineering complexities and facilitate rapid industrial-scale developments for the valorisation of plastic wastes and biomass. Therefore, operating co-HTL of biomass and plastics at moderate temperatures and low pressures to make sustainable fuels can deliver low processing costs and huge energy savings.

CRedit authorship contribution statement

Jude A. Onwudili: contributed to, Conceptualization, Methodology,

design, Project administration, Visualization, carried out laboratory, Investigation, Validation, presentation of the experimental data and paper writing (drafting, Writing – review & editing. Paul T. Williams: contributed to characterisation of catalysts, Project administration, Validation, and paper writing, Writing – review & editing, Both authors have read and agreed to the published version of the manuscript.

Declaration of competing interest

The authors declare that they have no known competing financial interests or personal relationships that could have appeared to influence the work reported in this paper.

Data availability

Data will be made available on request.

References

- Ahmadi, S., Reyhanitash, E., Yuan, Z., Rohani, S., Xu, C., 2017. Upgrading of fast pyrolysis oil via catalytic hydrodeoxygenation: effects of type of solvents. *Renew. Energy* 114 (Part B), 376–382. <https://doi.org/10.1016/j.renene.2017.07.041>, 2017.
- Alves, C.T., Onwudili, J.A., 2022. Screening of nickel and platinum catalysts for glycerol conversion to gas products in hydrothermal media. *Energies* 15, 7571. <https://doi.org/10.3390/en15207571>.
- Ansari, K.B., Arora, J.S., Chew, J.W., Dauenhauer, P.J., Mushrif, S.H., 2019. Fast Pyrolysis of cellulose, hemicellulose, and lignin: effect of operating temperature on bio-oil yield and composition and insights into the intrinsic pyrolysis chemistry. *Ind. Eng. Chem. Res.* 58 (35), 15838–15852. <https://doi.org/10.1021/acs.iecr.9b00920>, 2019.
- Bhaskar, T., Matsui, T., Kaneko, J., Uddin, M.A., Muto, A., Sakata, Y., 2002. Novel calcium-based sorbent (Ca-C) for the dehalogenation (Br, Cl) process during halogenated mixed plastic (PP/PE/PS/PVC and HIPS-Br) pyrolysis. *Green Chem.* 4, 372–375. <https://doi.org/10.1039/B203745A>.
- Capraris, B.D., Bracciale, M.P., Bavasso, I., Chen, G., Damizia, M., Genova, V., Marra, F., Paglia, L., Pulci, G., Scarsella, M., Tai, L., De Filippis, P., 2020. Unsupported Ni metal catalyst in hydrothermal liquefaction of oak wood: effect of catalyst surface modification. *Sci. Total Environ.* 709, 136215 <https://doi.org/10.1016/j.scitotenv.2019.136215>.
- Channiwala, S.A., Parikh, P.P., 2002. A unified correlation for estimating HHV of solid, liquid and gaseous fuels. *Fuel* 81 (8), 1051–1063. [https://doi.org/10.1016/S0016-2361\(01\)00131-4](https://doi.org/10.1016/S0016-2361(01)00131-4).
- Chen, W.-T., Jin, K., Linda Wang, N.-H., 2019. Use of supercritical water for the liquefaction of polypropylene into oil. *ACS Sustain. Chem. Eng.* 7, 3749–3758. <https://doi.org/10.1021/acssuschemeng.8B03841>.
- Cheng, S., Wei, L., Alsowij, M., Corbin, F., Boakye, E., Gu, Z., Raynie, D., 2017. Catalytic hydrothermal liquefaction (HTL) of biomass for bio-crude production using Ni/HZSM-5 catalysts. *AIMS Environ. Sci.* 4 (3), 417–430. <https://doi.org/10.3934/envirosci.2017.3.417>.
- Colnik, M., Kotnik, P., Knez, Ž., Škerget, M., 2022. Chemical recycling of polyolefins waste materials using supercritical water. *Polymers* 14, 4415. <https://doi.org/10.3390/polym14204415>.
- Elliott, D.C., Biller, P., Ross, A.B., Schmidt, A.J., Susanne, B., Jones, S.B., 2015. Hydrothermal liquefaction of biomass: developments from batch to continuous process. *Bioresour. Technol.* 178, 147–156. <https://doi.org/10.1016/j.biortech.2014.09.132>.
- Fan, Y., Prestigiacomo, C., Gong, M., Tietz, T., Hornung, U., Dahmen, N., 2022. Comparative investigation on the value-added products obtained from continuous and batch hydrothermal liquefaction of sewage sludge. *Front. Environ. Sci.* 10, 996353 <https://doi.org/10.3389/fenvs.2022.996353>.
- Faust, K., Denifl, P., Hapke, M., 2023. Recent advances in catalytic chemical recycling of polyolefins. *ChemCatChem* 15, e2023003. <https://doi.org/10.1002/cctc.202300310>.
- Fu, J., Lu, X., Savage, P.E., 2011. Hydrothermal decarboxylation and hydrogenation of fatty acids over Pt/C. *ChemSusChem* 4, 481–486. <https://doi.org/10.1002/cssc.201000370>.
- Geyer, R., Jambeck, J.R., Law, K.L., 2017. Production, use, and fate of all plastics ever made. *Sci. Adv.* 19 (7), e1700782 <https://doi.org/10.1126/sciadv.1700782>, 3.
- Gollakota, A.R.K., Kishore, N., Gu, S., 2018. A review on hydrothermal liquefaction of biomass. *Renew. Sustain. Energy Rev.* 81 (Part 1), 1378–1392. <https://doi.org/10.1016/j.rser.2017.05.178>.
- Green, S.K., Patet, R.E., Nikbin, N., Williams, C.L., Chang, C.-C., Yu, J., Gorte, R.J., Caratzoulas, S., Fan, W., Vlachos, D.G., Dauenhauer, P.J., 2016. Diels–Alder cycloaddition of 2-methylfuran and ethylene for renewable toluene. *Appl. Catal. B Environ.* 180, 487–496. <https://doi.org/10.1016/j.apcatb.2015.06.044>.
- Hongthong, S., Leese, H.S., Chuck, C.J., 2020a. Valorizing plastic-contaminated waste streams through the catalytic hydrothermal processing of polypropylene with lignocellulose. *ACS Omega* 5 (32), 20586–20598. <https://doi.org/10.1021/acsomega.0c02854>, 2020.

- Hongthong, S., Raikova, S., Leese, H.S., Chuck, C.J., 2020b. Co-processing of common plastics with pistachio hulls via hydrothermal liquefaction. *Waste Manag.* 102, 351–361. <https://doi.org/10.1016/j.wasman.2019.11.003>.
- Jahirul, M.I., Rasul, M.G., Chowdhury, A.A., Ashwath, N., 2012. Biofuels production through biomass pyrolysis - A technological review. *Energies* 5, 4952–5001. <https://doi.org/10.3390/en5124952>.
- Jin, K., Vozka, P., Gentilcore, C., Kilaz, G., Wang, N.-H.L., 2021. Low-pressure hydrothermal processing of mixed polyolefin wastes into clean fuels. *Fuel* 294, 120505. <https://doi.org/10.1016/j.fuel.2021.120505>.
- Kohansal, K., Sharma, K., Toor, S.S., Sanchez, E.L., Zimmermann, J., Rosendahl, L.A., Pedersen, T.H., 2021. Bio-crude production improvement during hydrothermal liquefaction of biopulp by simultaneous application of alkali catalysts and aqueous phase recirculation. *Energies* 14, 4492. <https://doi.org/10.3390/en14154492>.
- Kruse, A., Dinjus, E., 2005. Influence of salts during hydrothermal biomass gasification: the role of the catalysed water-gas shift reaction. *Z. Phys. Chem.* 219, 341–366. <https://doi.org/10.1524/zpch.219.3.341.59177>.
- Lachos-Perez, D., Torres-Mayanga, P.C., Abaide, E.R., Zabot, G.L., De Castilhos, F., 2022. Hydrothermal carbonization and liquefaction: differences, progress, challenges, and opportunities. *Bioresour. Technol.* 343, 126084. <https://doi.org/10.1016/j.biortech.2021.126084>, 2022.
- Laredo, G.C., Reza, J., Ruiz, E.M., 2023. Hydrothermal liquefaction processes for plastics recycling: a review. *Cleaner Chem. Eng.* 5, 100094. <https://doi.org/10.1016/j.cce.2023.100094>.
- Liu, W.-J., Yu, H.-Q., 2022. Thermochemical conversion of lignocellulosic biomass into mass producible fuels: emerging technology progress and environmental sustainability evaluation. *ACS Environ. Au* 2, 98–114. <https://doi.org/10.1021/acsenvironau.1c00025>.
- Luna-Murillo, B., Pala, M., Paioni, A.L., Baldus, M., Ronsse, F., Prins, W., Bruijninx, P.C. A., Weckhuysen, B.M., 2021. Catalytic fast pyrolysis of biomass: catalyst characterization reveals the feed-dependent deactivation of a technical ZSM-5-based catalyst. *ACS Sustain. Chem. Eng.* 9, 291–304. <https://doi.org/10.1021/acssuschemeng.0c07153>.
- Minowa, T., Zhen, F., Ogi, T., 1998. Cellulose decomposition in hot-compressed water with alkali or nickel catalyst. *J. Supercrit. Fluids* 13 (1–3), 253–259. [https://doi.org/10.1016/S0896-8446\(98\)00059-X](https://doi.org/10.1016/S0896-8446(98)00059-X).
- Muhammad, C., Onwudili, J.A., Williams, P.T., 2015. Thermal degradation of real-world waste plastics and simulated mixed plastics in a two-stage pyrolysis-catalysis reactor for fuel production. *Energy Fuel.* 29, 2601–2609. <https://doi.org/10.1021/EF502749H>.
- Mukundan, S., Wagner, J.L., Annamalai, P.K., Ravindran, D.S., Krishnapillai, G.K., Beltramini, J., 2022. Hydrothermal co-liquefaction of biomass and plastic wastes into biofuel: study on catalyst property, product distribution and synergistic effects. *Fuel Process. Technol.* 238, 107523. <https://doi.org/10.1016/j.fuproc.2022.107523>.
- Onsager, O.T., Brownrigg, M.S., Lodeng, R., 1996. Hydrogen production from water and CO via alkali metal formate salts. *Int. J. Hydrogen Energy* 21, 883–885. [https://doi.org/10.1016/0360-3199\(96\)00031-6](https://doi.org/10.1016/0360-3199(96)00031-6).
- Onwudili, J.A., Scaldaferrì, C.A., 2023. Catalytic upgrading of intermediate pyrolysis bio-oil to hydrocarbon-rich liquid biofuel via a novel two-stage solvent-assisted process. *Fuel* 352, 129015. <https://doi.org/10.1016/j.fuel.2023.129015>.
- Onwudili, J.A., Insura, N., Williams, P.T., 2009. Composition of products from the pyrolysis of polyethylene and polystyrene in a closed batch reactor: effects of temperature and residence time. *J. Anal. Appl. Pyrol.* 86, 293–303. <https://doi.org/10.1016/j.jaap.2009.07.008>.
- Onwudili, J.A., Williams, P.T., 2007. Reaction mechanisms for the hydrothermal oxidation of petroleum derived aromatic and aliphatic hydrocarbons. *J. Supercrit. Fluids* 43 (1), 81–90. <https://doi.org/10.1016/j.supflu.2007.04.011>.
- Özgen, A.Y., 2020. Conversion of Biomass to organic acids by liquefaction reactions under subcritical conditions. *Front. Chem.* 8, 1–14. <https://doi.org/10.3389/fchem.2020.00024>.
- Razaq, I., Simons, K.E., Onwudili, J.A., 2021. Parametric study of Pt/C-catalysed hydrothermal decarboxylation of butyric acid as a potential route for biopropane production. *Energies* 14, 3316. <https://doi.org/10.3390/en14113316>.
- Sebestyén, Z., Blazsó, M., Jakab, E., Miskolczi, N., Bozi, J., Czégény, Z., 2022. Thermocatalytic studies on a mixture of plastic waste and biomass. *J. Therm. Anal. Calorim.* 147, 6259–6270. <https://doi.org/10.1007/s10973-021-10962-5>.
- Seshasayee, M.S., Savage, P.E., 2021. Synergistic interactions during hydrothermal liquefaction of plastics and biomolecules. *Chem. Eng. J.* 417, 129268. <https://doi.org/10.1016/j.cej.2021.129268>.
- Sharma, K., Castello, D., Haider, M.S., Pedersen, T.H., Rosendahl, L.A., 2021. Continuous co-processing of HTL bio-oil with renewable feed for drop-in biofuels production for sustainable refinery processes. *Fuel* 306, 121579. <https://doi.org/10.1016/j.fuel.2021.121579>.
- Sogancioglu, M., Yel, E., Ahmetli, G., 2017. Pyrolysis of waste high density polyethylene (HDPE) and low-density polyethylene (LDPE) plastics and production of epoxy composites with their pyrolysis chars. *J. Clean. Prod.* 165, 369–381. <https://doi.org/10.1016/j.jclepro.2017.07.157>.
- Stanton, A.R., Lisa, K., Mukarakate, C., Nimlos, M.R., 2018. Role of biopolymers in the deactivation of ZSM-5 during catalytic fast pyrolysis of biomass. *ACS Sustain. Chem. Eng.* 6, 10030–10038. <https://doi.org/10.1021/acssuschemeng.8b01333>.
- Wagner, J., Bransgrove, R., Beacham, T.A., Allen, M.J., Meixner, K., Drosig, B., Ting, V.P., Chuck, C.J., 2016. Co-production of bio-oil and propylene through the hydrothermal liquefaction of polyhydroxybutyrate producing cyanobacteria. *Bioresour. Technol.* 207, 166–174. <https://doi.org/10.1016/j.biortech.2016.01.114>.
- Watson, J., Wang, T., Si, B., Chen, W.T., Aierzhati, A., Zhang, Y., 2020. Valorization of hydrothermal liquefaction aqueous phase: pathways towards commercial viability. *Prog. Energy Combust. Sci.* 77, 100819. <https://doi.org/10.1016/j.pecs.2019.100819>.
- Williams, P.T., Onwudili, J., 2006. Subcritical and supercritical water gasification of cellulose, starch, glucose, and biomass waste. *Energy Fuel.* 20, 1259–1265. <https://doi.org/10.1021/ef0503055>.
- Xu, X., Zhang, C., Liu, Y., Zhai, Y., Zhang, R., 2013. Two-step catalytic hydrodeoxygenation of fast pyrolysis oil to hydrocarbon liquid fuels. *Chemosphere* 93 (4), 652–660. <https://doi.org/10.1016/j.chemosphere.2013.06.060>.
- Yao, G., Duo, J., Jin, B., Zhong, H., Lyu, L., Ma, Z., Jin, F., 2017. Highly efficient and autocatalytic reduction of NaHCO₃ into formate by in situ hydrogen from water splitting with metal/metal oxide redox cycle. *J. Energy Chem.* 26 (5), 881–890. <https://doi.org/10.1016/j.jechem.2017.08.011>.
- Yuan, X., Cao, H., Li, H., Zeng, G., Tong, J., Wang, L., 2009. Quantitative and qualitative analysis of products formed during co-liquefaction of biomass and synthetic polymer mixtures in sub- and supercritical water. *Fuel Process. Technol.* 90, 428–434. <https://doi.org/10.1016/j.fuproc.2008.11.005>.
- Zhang, X.-S., Yang, G.-X., Jiang, H., Liu, W.-J., Ding, H.-S., 2013. Mass production of chemicals from biomass-derived oil by directly atmospheric distillation coupled with co-pyrolysis. *Sci. Rep.* 3, 1120. <https://doi.org/10.1038/srep01120>.